MAGNETORESISTANCE AND HALL EFFECT CAUSED BY BERRY CURVATURE IN $Sr_2FeMoO_{6-\delta}$ DOUBLE PEROVSKITE

S. M. Konoplyuk, M. M. Krupa
Institute of Magnetism of NASU and MESU,
Vernadsky blvd., 36-b, Kyiv, UA–03142, Ukraine
e-mail: ksm@imag.kiev.ua

(Received 30 October 2023; in final form 18 November 2023; accepted 04 December 2023;
published online 23 December 2023)

The paper focuses on transport properties of double perovskite $Sr_2FeMoO_{6-\delta}$, which were studied experimentally and using first principles calculations. The strontium ferromolybdate specimens were prepared using citrate-gel method followed by compacting and thermal treatment at different regimes. The Hall effect was calculated using Quantum Espresso and Wannier90 software packages.

The study confirmed high sensitivity of Sr_2FeMoO_6 to the processing parameters such as pressure and temperature of powder compacting as well as the temperature and duration of the subsequent annealing in Ar/O_2 atmosphere. The optimal regime of compacting to avoid cracking involved pressing under 4 GPa at $T = 800$ K. Further heat treatment of the compacted specimens in Ar/O_2 atmosphere has shown that three types of electric conductivity, namely metallic, semiconducting and mixed one can be realized in the Sr_2FeMoO_6 specimens. The highest magnitude of magnetoresistance was found in the semiconducting specimen (about 44%), while the specimen of metallic type demonstrated magnetoresistance of about 21%. The elevated values of magnetoresistance in the semiconducting specimen were achieved due to conduction mechanism related to tunneling through intergrain dielectric layers formed by secondary $SrMoO_4$ phase.

The Hall effect was computed by constructing the Hamiltonian in the maximally-localized Wannier functions basis. Calculations of the Berry curvature, which is the origin of the high intrinsic Hall effect showed that its highest magnitudes concentrate near avoided band crossings gapped out due to spin-orbit coupling. The Hall conductivity calculated by integrating the Berry curvature over all occupied bands was found to be ~ 22 S/cm.

Key words: Sr_2FeMoO_6, electric resistance, magnetoresistance, Hall effect, Berry curvature.

DOI: https://doi.org/10.30970/jps.27.4703

I. INTRODUCTION

Double perovskite metal oxides comprise a class of materials whose crystal structure can be described as $A_2BB'O_6$ where A is a rare earth element, B is a transition metal. These materials attract attention due to technological prospectives related to their excellent transport properties, improved oxygen kinetics, high chemical stability, and compositional flexibility.

Sr_2FeMoO_6 may be the most studied double perovskite ceramic material. High Curie temperature and full spin polarization [1] suggest its utilization in magnetic tunnel junctions [2], spin valves [3], although other application options such as anode material in solid fuel cells [4], magnetocaloric working body [5], active layer in solar cells [6] also have great practical potential. Sr_2FeMoO_6 can be fabricated in different ways, including by using solid state and sol-gel methods [7, 8], melting of constituent elements [9] and so on. In the case of spintronic applications, proper thermal treatment in addition to effective synthesis method is required to gain prescribed transport properties. In this work, different synthesis and thermal treatment regimes were tested to improve magnetoresistance of $Sr_2FeMoO_{6-\delta}$. Our tasks involved forming dielectric layers between adjacent Sr_2FeMoO_6 grains in order to provide the tunneling magnetoresistance mechanism, and determining the magnetoresistance of samples synthesized. Besides, the Hall effect was studied to evaluate the prospectives of $Sr_2FeMoO_{6-\delta}$ for application in magnetic sensors.

II. MATERIALS AND METHODS

$Sr_2FeMoO_{6-\delta}$ powders were prepared by using the citrate-gel method [10] from the strontium nitrate $Sr(NO_3)_2$, iron nitrate $Fe(NO_3)_3{\cdot}9H_2O$, ammonium molybdate $(NH_4)_6Mo_7O_{24}$, and citric acid monohydrate $C_6H_8O_7{\cdot}H_2O$ components. Then the synthesized $Sr_2FeMoO_{6-\delta}$ powders were pressed into tablets with a diameter of 10 mm under different pressures and temperatures. The parameters of pressing varied over the range 1–4 GPa for pressure and 300–1100 K for temperature to select those which would allow avoiding the formation of cracks or any secondary phase except Sr_2FeMoO_6. Then the annealing of the specimens compacted at selected temperatures and pressures was carried out in mixed Ar/O_2 atmosphere to form dielectric shells on the grain surface by controllable oxidation. The electrical resistivity and magnetoresistance were measured by using four terminal method in the temperature range of 4.2–300 K. Magnetoresistance was determined according to the expression $MR(\%) = 100(R(H,T) - R(0,T))/R(0,T)$. It is worth mentioning that the computations of the Hall effect were performed on the premise of a tetragonal $I4/m$

structure of Sr_2FeMoO_6 with ferrimagnetic ordering. The intrinsic Hall conductivity was calculated by using the method of maximally-localized Wannier functions using Wannier90 code [11]. The Quantum Espresso software package [12] was employed to find ground state Bloch functions required for Wannier90 computations. The Quantum Espresso provided DFT calculations using PBEsol pseudopotentials for Perdew–Burke–Ernzerhoff functional on Monkhorst–Pack k-points grid.

III. RESULTS AND DISCUSSION

The consolidation of nanopowders at different pressures and temperatures $T \leq 500$ K produced cracks in the samples. The samples compacted under a pressure of 1 GPa and temperature of 300 K were found to be weakly semiconducting, which indicated the presence of weak intergranular bonds. As the pressure of compacting was raised up to 3 GPa at room temperature, a decrease in resistivity and the change of its temperature dependent behavior from semiconducting to metallic type above 150 K were observed. In these samples, the magnetoresistance reached only 12% in the magnetic field of 10 T at 10 K. Thus, to improve intergranular bonds and increase magnetoresistance, the pressure and temperature of compacting should be increased.

Increasing the temperature during the pressing of $Sr_2FeMoO_{6-\delta}$ to $T = 800$ K resulted in a slightly denser microstructure of the tablets and almost complete absence of microcracks. Densifying the samples continued as consolidation pressure was raised to 4 GPa. It was accompanied by a drop in the resistivity in the whole temperature interval of 4.2–300 K. An increase in the temperature of compacting to 1100 K led to phase segregation with the appearance of dispersed Fe and $SrMoO_4$ inclusions.

The testing of different compacting regimes revealed that the tablets without cracks and secondary phases should be produced under the pressure of 4 GPa at $T = 800$ K for 1 min.

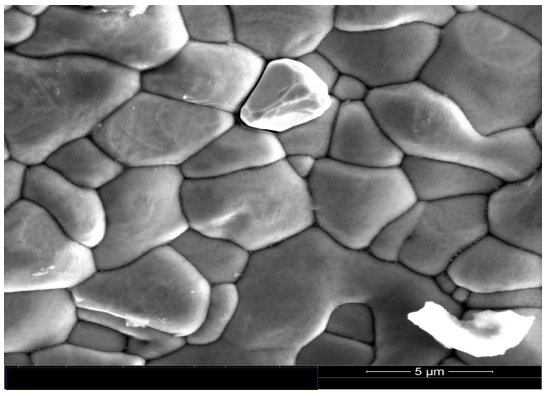

Fig. 1. Scanning electron microscopy image of the annealed $Sr_2FeMoO_{6-\delta}$ specimen

After fabrication with the abovementioned selected parameters, the tablets were annealed for varying times to form dielectric shells around $Sr_2FeMoO_{6-\delta}$ grains. A series of the samples DP-1, DP-2, DP-3 underwent thermal treatment followed by measurements of their transport properties.

The DP-2 and DP-3 were annealed at $T = 700$ K and $p(O_2) = 10$ Pa for 3 and 5 hours, while DP-1 did not undergo any heat treatment. Fig. 1 shows the microstructure of the tablet after annealing.

The size of the grains is between 1 and 7 μm. The structure is well compacted, without cracks and voids. This was achieved by using properly chosen pressing parameters due to grain growth during annealing.

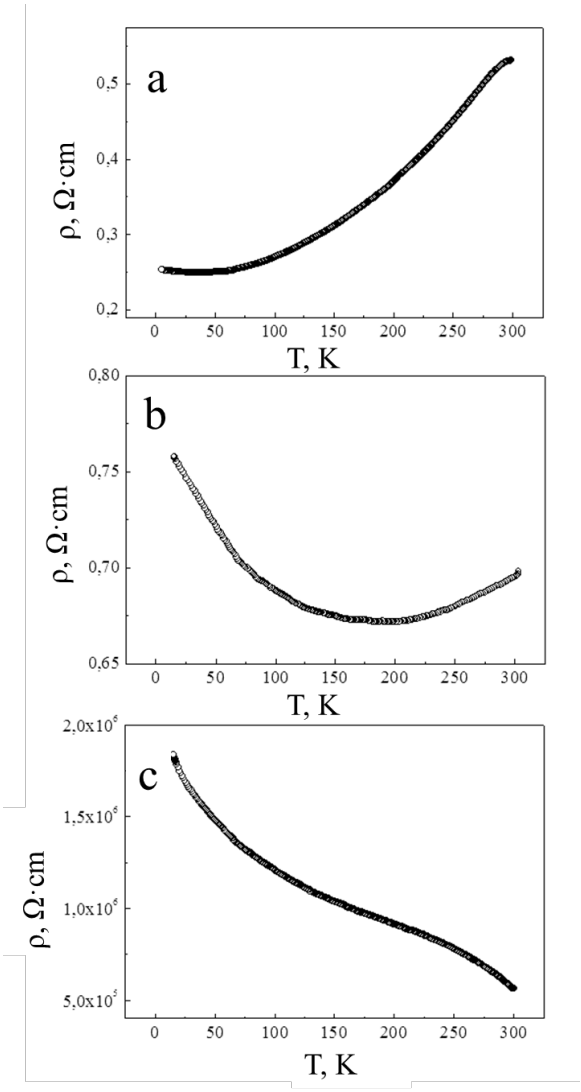

Fig. 2. Electrical conductivity of $Sr_2FeMoO_{6-\delta}$ samples a) without additional annealing, b) annealed in Ar/O_2 mixture at 700 K for 3 hours, c) annealed in Ar/O_2 mixture at 700 K for 5 hours

Influence of annealing on the transport properties of $Sr_2FeMoO_{6-\delta}$ was studied in the temperature interval from 4.2 to 300 K (Fig. 2). The results displayed in $\rho(T)$ dependencies indicate that the DP-1, DP-2, DP-3 samples have different conduction mechanisms. DP-1 has a positive slope of the temperature coefficient of resistance ($d\rho/dT$) and metallic conductivity throughout

the entire temperature range studied (Fig. 2,a). The DP-2 sample is characterized by a change in the sign of $d\rho/dT$ from positive to negative at about 200 K on cooling (Fig. 2,b). The DP-3 sample has a higher electrical resistivity $\rho = 579431$ Ohm·cm than the DP-1 and the DP-2 samples with $\rho = 0.537$ Ohm·cm and $\rho = 0.696$ Ohm·cm at 300 K, respectively.

The DP-3 demonstrated a well-defined semiconductor conductivity with $d\rho/dT < 0$ (Fig. 2,c). In order to find the reasons for this behavior, the X-ray diffraction (XRD) measurements of the DP-3 specimen were performed. The small peaks (112), (004), (200), which belong to dielectric $SrMoO_4$ in addition to the main reflections of Sr_2FeMoO_6 phase, were identified in the diffractogram (Fig. 3).

According to the XRD analysis, the concentration of $SrMoO_4$ phase was below 5.4% in the DP-3. The XRD analysis also revealed that the parameters of the crystal lattice and the concentration of antisite defects remained unchanged after annealing. Taking into account that magnetizations of all the samples studied were almost identical, one can suggest that the $SrMoO_4$ phase appears mostly on the surface of $Sr_2FeMoO_{6-\delta}$ grains in the form of thin shells, thus creating dielectric barriers between them. These barriers affect conductivity of the DP-3 sample as well as its magnetoresistance.

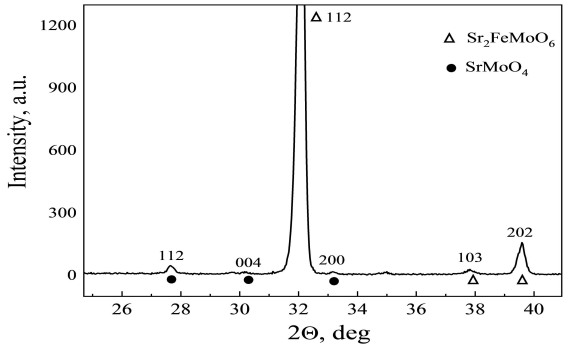

Fig. 3. The XRD pattern of the DP-3 sample demonstrating appearance of $SrMoO_4$ phase after annealing at 700 K for 5 hours

As it follows from Fig. 4, the magnetoresistance of all the samples is negative in the whole temperature interval studied and decreases with temperature. Its maximum value reaches 21.2% in the DP-1 at $B = 10$ T and $T = 10$ K. MR increases to 26.1% in the DP-2 where traces of $SrMoO_4$ were detected by using the X-ray fluorescence method. Further increase of the annealing time to 5 hours facilitates the formation of intergranular dielectric layers enhancing magnetoresistance to 43.6% in the DP-3 sample. The maximum growth of magnetoresistance occurs at $B \leq 0.2$ T. As the magnetic field increases to 10 T, magnetoresistance tends towards saturation. Magnetoresistance of $Sr_2FeMoO_{6-\delta}$ with dielectric shells can be described based on the model [13], wherein the probability of tunneling electrons between grains depends on the mutual orientation of their magnetic moments. In this case, the tunneling current depends on the angle between the magnetic moments of adjacent grains: $\rho - \rho_S \sim 1 - \cos(\theta_{ij})$. This can be averaged over all the nearest neighboring grains i and j. Then, the following expression can be written:

$$(\rho - \rho_S) \sim \langle (1 - \cos\theta_{ij}) \rangle_{ij} = 1 - \langle \cos\theta_i \rangle_i^2 = 1 - (M/M_S)^2 ,$$

where M_S is the saturation magnetization, ρ_S is resistivity at the saturation. Taking into account the spin polarization of electrons P, the expression for magnetoresistance MR is

$$MR = -P^2(M/M_S)^2/(1 + P^2(M/M_S)^2),$$

which in the case of $Sr_2FeMoO_{6-\delta}$ with almost 100% spin polarization becomes $MR \sim (M/M_S)^2$ in accordance with experimental results.

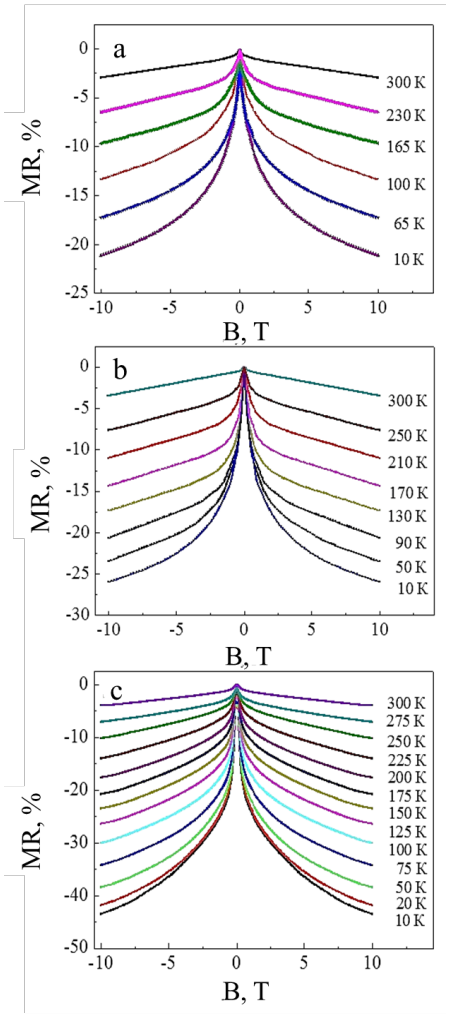

Fig. 4. Magnetoresistance of $Sr_2FeMoO_{6-\delta}$ samples a) without additional annealing, b) annealed in Ar/O_2 mixture at 700 K for 3 hours, c) annealed in Ar/ O_2 mixture at 700 K for 5 hours

The Hall effect (HE) in magnetic materials is composed of two parts, ordinary HE and anomalous HE

$$\rho_H = \rho_{ord} + \rho_{an} = R_{ord}B + R_{an}M.$$

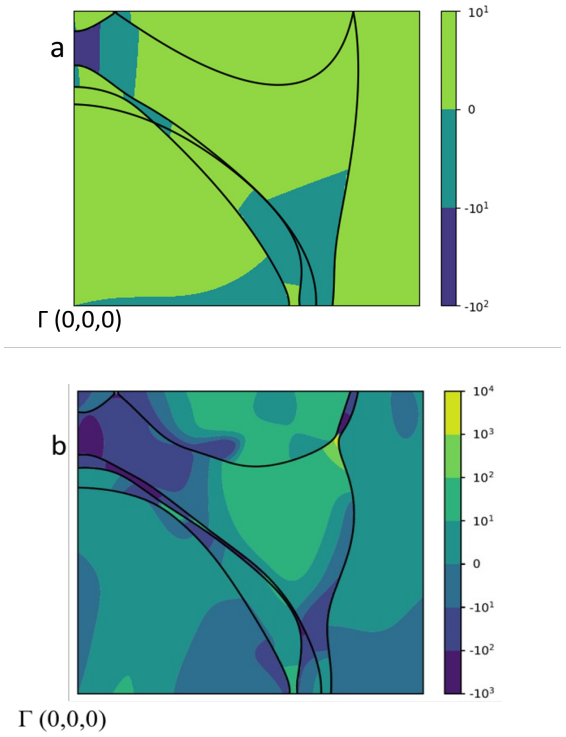

Fig. 5. Plot of Berry curvature $-\mathbf{\Omega}_z = -\mathbf{\Omega}_{xy}$ distributed over $k_y = 0$ plane a) without spin-orbit coupling, b) with spin-orbit coupling

In their turn, three different mechanisms contribute to the anomalous HE including the intrinsic one, side-jump, and skew scattering ones. The former mechanism depends only on the band structure of a perfect crystal and therefore can be calculated within the framework of the ab-initio approach. The intrinsic anomalous HE is greatly enhanced by spin-orbit coupling [14], which is proportional to the fourth power of nucleus charge and hence is stronger in alloys with heavy elements. Although Sr_2FeMoO_6 does not have such a strong spin-orbit coupling as manganites or spinels have, its conductivity of about 10^4 $(\text{Ohm}\cdot\text{cm})^{-1}$ may allow classifying Sr_2FeMoO_6 as an alloys with scattering-independent conductivity $(10^4 - 10^6\ (\text{Ohm}\cdot\text{cm})^{-1})$, wherein the intrinsic regime of anomalous HE is the dominant one [15].

The intrinsic anomalous HE is closely related to the Berry curvature [16], which plays the role of a fictitious magnetic field in momentum k-space and provides an additional term to the expression for the electron wavepacket group velocity

$$\mathbf{v}_n(\mathbf{k}) = \frac{\partial \varepsilon_n(\mathbf{k})}{\hbar \partial \mathbf{k}} - \frac{e}{\hbar}\mathbf{E} \times \mathbf{\Omega}_n(\mathbf{k}), \qquad (1)$$

where the Berry curvature of the n-th band $\mathbf{\Omega}_n(\mathbf{k}) = i\langle \nabla_{\mathbf{k}} u_n(\mathbf{k}) | \times | \nabla_{\mathbf{k}} u_n(\mathbf{k}) \rangle$,

$\mathbf{E}$ is electric field, $u_n(\mathbf{k})$ are periodic Bloch functions. In the matrix representation

$$\mathbf{\Omega}_{n,\alpha\beta}(\mathbf{k}) = -2\Im\langle \nabla_{k_\alpha} u_n(\mathbf{k}) | \nabla_{k_\beta} u_n(\mathbf{k}) \rangle, \qquad (2)$$

where α and β are Cartesian coordinates.

The second term in Eq. (1) is a component of electron velocity perpendicular to the applied electric field, which is responsible for the Hall voltage. Figure 5 shows the heat map of the Berry curvature in Sr_2FeMoO_6 distributed over the plane $k_y = 0$ in the Brillouin zone of FCT lattice. The lines mark the intersection of the bands with the Fermi surface. The minority spin band crossings seen in Fig. 5,a, are protected by mirror symmetry. This symmetry is broken by spin-orbit coupling, which lifts the band degeneracy (Fig. 5,b). As is seen, spin-orbit interaction enhances the Berry curvature by several orders, especially near the avoided crossings.

In order to determine the intrinsic Hall conductivity, the Kubo–Greenwood formulae for interband optical conductivity in dc limit was used.

$$\sigma_{xy} = -\frac{e^2}{\hbar V N}\sum_{nk} f(\varepsilon_{nk}\mathbf{\Omega}_{n,xy}(\mathbf{k}), \qquad (3)$$

where V is a cell volume, $f(\varepsilon_{nk})$ is the Fermi–Dirac distribution function. It should be noted that the sum in Eq. (3) runs only over occupied states. Finally, calculations based on the abovementioned formula yielded 22 $\text{Ohm}^{-1}\cdot\text{cm}^{-1}$ for the intrinsic anomalous Hall conductivity of Sr_2FeMoO_6. Although this result is far from the best ones, the Hall effect produced by the intrinsic Berry curvature depends on the band structure of a perfect crystal and therefore can be improved by variation of the composition through additions of doping elements.

IV. CONCLUSIONS

- Optimal conditions for compacting $Sr_2FeMoO_{6-\delta}$ powders required to form a dense structure without microcracks include temperature of 800 K and pressure of 4 GPa;
- Annealing $Sr_2FeMoO_{6-\delta}$ pellets in Ar/O_2 flow at the temperature of 700 K facilitates the formation of the dielectric $SrMoO_4$ phase changing the conduction mechanism from metallic type to semiconducting one;
- The sample after additional annealing demonstrates enhanced magnetoresistance (from 21.2% to 43.6%) due to the intergrain tunneling through dielectric $SrMoO_4$ layers between $Sr_2FeMoO_{6-\delta}$ grains;
- In Sr_2FeMoO_6, the intrinsic anomalous Hall conductivity σ_{xy} due to the Berry curvature $\mathbf{\Omega}_z$ is about 22 S/cm.

[1] D. D. Sarma, P. Mahadevan, T. Saha-Dasgupta, S. Ray, A. Kumar, Phys. Rev. Lett. **85**, 2549 (2000); https://doi.org/10.1103/PhysRevLett.85.2549.
[2] T. Fix *et al.*, J. Appl. Phys. **99**, 08J107 (2006); https://doi.org/10.1063/1.2170070.
[3] D. Yang *et al.*, Ceram. Int. **45**, 10072 (2019); https://doi.org/10.1016/j.ceramint.2019.02.053.
[4] M. K. Rath, K. T Lee, Electrochim. Acta **212**, 678 (2016); https://doi.org/10.1016/j.electacta.2016.07.037.
[5] M. S. Anwar, I. Hussain, B. H. Koo, Mater. Lett. **181**, 56 (2016); https://doi.org/10.1016/j.matlet.2016.06.011.
[6] Z. Wang, Y.Tian, Y. Li, J. Power Sources **196**, 6104 (2011); https://doi.org/10.1016/j.jpowsour.2011.03.053.
[7] B. Jurca, J. Berthon, N. Dragoe, P. Berthet, J. Alloys Compd. **474**, 416 (2009); https://doi.org/10.1016/j.jallcom.2008.06.100.
[8] M. Cernea *et al.*, J. Eur. Ceram. Soc. **33**, 2483 (2013); https://doi.org/10.1016/j.jeurceramsoc.2013.03.026.
[9] Y. Moritomo *et al.*, J. Phys. Soc. Jpn. **69**, 1723 (2000); https://doi.org/10.1143/JPSJ.69.1723.
[10] M. M. Krupa, Y. B. Skirta, A. Kravets, S. M. Konoplyuk, Appl. Nanosci. **13**, 6887 (2023); https://doi.org/10.1007/s13204-023-02807-4.
[11] G. Pizzi *et al.*, J. Phys. Condens. Matter **32**, 165902 (2020); https://doi.org/10.1088/1361-648X/ab51ff.
[12] P. Giannozzi *et al.*, J. Phys. Condens. Matter **21**, 395502 (2009); https://doi.org/10.1088/0953-8984/21/39/395502.
[13] M. Julliere, Phys. Lett. A **54**, 225 (1975); https://doi.org/10.1016/0375-9601(75)90174-7.
[14] J. B. Goodenough, Phys. Rev. **171**, 466 (1968); https://doi.org/10.1103/PhysRev.171.466.
[15] N. Nagaosa, J. Sinova, S. Onoda, A. H. MacDonald, N. P. Ong, Rev. Mod. Phys. **82**, 1539 (2010); https://doi.org/10.1103/RevModPhys.82.1539.
[16] D. Xiao, M. C. Chang, Q. Niu, Rev. Mod. Phys. **82**, 1959 (2010); https://doi.org/10.1103/RevModPhys.82.1959.

МАГНІТООПІР ТА ЕФЕКТ ГОЛЛА, ВИКЛИКАНИЙ КРИВИЗНОЮ БЕРРІ В ПОДВІЙНОМУ ПЕРОВСКІТІ $Sr_2FeMoO_{6-\delta}$

С. М. Коноплюк, М. М. Крупа
Інститут магнетизму НАН України та МОН України,
бульв. Вернадського 36-б, 03142, Київ, Україна

Транспортні властивості подвійного перовскіту $Sr_2FeMoO_{6-\delta}$ досліджували експериментально та з використанням першопринципних розрахунків. Зразки феромолібдату стронцію готували цитратно-гелевим методом з подальшим пресуванням і термообробкою в різних режимах. Ефект Голла розраховували за допомогою програмних пакетів Quantum Espresso та Wannier90. Дослідження підтвердили високу чутливість властивостей $Sr_2FeMoO_{6-\delta}$ до таких параметрів обробки, як тиск і температура пресування порошку, а також до температури й тривалості подальшого відпалу в змішаній атмосфері аргону та кисню. Установлено, що оптимальний режим пресування, який давав змогу уникнути розтріскування зразків, досягався за тиску 4 ГПа та температури 800 K. Подальша термічна обробка пресованих зразків у змішаній атмосфері Ar та O_2 показала, що в $Sr_2FeMoO_{6-\delta}$ можна отримати три типи електропровідності: металеву, напівпровідникову та змішану.

Найбільшу величину магнітоопору виявлено в напівпровідникового зразка (близько 44%), тоді як зразок металевого типу продемонстрував магнітоопір близько 21%. Підвищених значень магнітоопору в напівпровідниковому зразку досягнуто за рахунок механізму провідності, пов'язаного з тунелюванням через міжзеренні діелектричні шари, утворені вторинною фазою $SrMoO_4$. Внутрішню частину аномального ефекту Голла обчислено за допомогою побудови гамільтоніана в базисі максимально локалізованих функцій Ваньє. Розрахунки кривизни Беррі, яка є причиною внутрішнього ефекту Голла, показали, що її найбільші значення досягаються поблизу уникнутих перетинів зон за врахування спін-орбітального зв'язку. Провідність Голла розрахована інтеґруванням кривизни Беррі по всіх зайнятих станах ~ 22 S/см.

Ключові слова: Sr_2FeMoO_6, електроопір, магнітоопір, ефект Голла, кривизна Беррі.